Int J CARS (2010) 5:237–249
DOI 10.1007/s11548-009-0389-8

ORIGINAL ARTICLE

Classification and numbering of teeth in multi-slice CT images using wavelet-Fourier descriptor

Mohammad Hosntalab · Reza Aghaeizadeh Zoroofi · Ali Abbaspour Tehrani-Fard · Gholamreza Shirani

Received: 10 January 2009 / Accepted: 21 June 2009 / Published online: 29 July 2009

Abstract
Purpose Teeth arrangement is essential in face ergonomics and healthiness. In addition, they play key roles in forensic medicine. Various computer-assisted procedures for medical application in quantitative dentistry require automatic classification and numbering of teeth in dental images.
Method In this paper, we propose a multi-stage technique to classify teeth in multi-slice CT (MSCT) images. The proposed algorithm consists of the following three stages: segmentation, feature extraction and classification. We segment the teeth by employing several techniques including Otsu thresholding, morphological operations, panoramic re-sampling and variational level set. In the feature extraction stage, we follow a multi-resolution approach utilizing wavelet-Fourier descriptor (WFD) together with a centroid distance signature. We compute the feature vector of each tooth by employing the slice associated with largest tooth tissues. The feature vectors are employed for classification in the third stage. We perform teeth classification by a conventional supervised classifier. We employ a feed-forward neural network classifier to discriminate different teeth from each other.
Results The performance of the proposed method was evaluated in the presence of 30 different MSCT data sets including 804 teeth. We compare classification results of the WFD technique with Fourier descriptor (FD) and wavelet descriptor (WD) techniques. We also investigate the invariance properties of the WFD technique. Experimental results reveal the effectiveness of the proposed method.
Conclusion We provided an integrated solution for teeth classification in multi-slice CT datasets. In this regard, suggested segmentation technique was successful to separate teeth from each other. The employed WFD approach was successful to discriminate and numbering of the teeth in the presence of missing teeth. The solution is independent of anatomical information such as knowing the sequence of teeth and the location of each tooth in the jaw.

Keywords Teeth classification · Wavelet-Fourier descriptors · Teeth segmentation · Variational level set · Dental CT

M. Hosntalab (✉) · A. Abbaspour Tehrani-Fard
Faculty of Engineering, Science and Research Branch, Islamic Azad University (IAU), Tehran, Iran
e-mail: mhosntalab@yahoo.com

A. Abbaspour Tehrani-Fard
e-mail: abbaspour@sharif.edu

R. Aghaeizadeh Zoroofi
Control and Intelligent Processing Center of Excellence, School of Electrical and Computer Engineering, College of Engineering, University of Tehran, Tehran, Iran
e-mail: zoroofi@ut.ac.ir

G. Shirani
Oral and Maxillofacial Surgery Department, Faculty of Dentistry Medical Science of Tehran University, Tehran, Iran
e-mail: ghr_shirani@yahoo.com

Introduction

Teeth are one of the most important anatomical structures in the face, which have critical roles in mastication, phonetics and esthetics [1]. In modern dentistry, computer-assisted procedures such as surgical preoperative planning, intra-operative navigation and post-operative assessments in common dental procedures such as tooth restoration, mechanized dental implants and removable dentures, orthodontic planning and orthognathic surgery are currently rising due to the growing public awareness of the role of teeth [2–6].

Teeth are the hardest tissues in the human body and play key roles in forensic medicine. In this regard, a postmortem (PM) record is compared against antemortem (AM) records pertaining to some presumed identity. Teeth are unique in identification of deceased persons where other conventional biometric features for authentication such as face, fingerprint, iris, etc. are not applicable. Under severe circumstances, dental features are regarded as the best candidates for PM biometric identification. Teeth not only represent a suitable repository for distinctive and identifying features, but also survive in most PM events that can disrupt or change other body tissues. Typical examples are airplane crashes, fire accidents, or if identification is being attempted more than a couple of weeks postmortem [7–10].

Various image-based computer-assisted procedures in quantitative dentistry require automatic classification and numbering of teeth. For example, a human identification system in forensic dentistry requires automatic recognition of teeth in dental images. In this case, developing automated systems for comparing identical teeth may improve the speed and robustness of the system. Moreover, proposing methods for dental recognition and teeth arrangement may effectively fulfill the demands of specialists for the routine dental procedures, maxillofacial surgical applications and teeth generic modelling.

For years, dental X-ray plays an important role, for most dental practitioners, as the basis of medical imaging [11]. In the previous works, dental recognition mostly applied conventional dental radiography such as panoramic, perapical and bitewing images. In [12], using bitewing images, a method were proposed to obtain the indices of teeth. Classification of the teeth was performed by utilizing Fourier descriptors (FDs). FDs were derived from complex coordinates and centroid distance shape signature. The method was only developed for classification of molar and premolar in bitewing images with no missing teeth. In [13], a method based on atlas registration was proposed. They utilized a Hidden Markov Model (HMM) and employed different feature sets in their approach. The methods proposed in [12,13] were based on anatomical information such as knowing the sequence of teeth, and the approximated location of each tooth in the mouth with respect to each other.

Nowadays, computed tomography (CT) has become the most frequently used imaging modality to provide clinical data sets for different medical applications and clinical studies ranging from 3D visualization to quantitative studies [14]. A few studies describing the general use of CT for forensic identification are available in the literature [15–18]. These studies revealed that CT of the dentition might be a practicable and reliable tool for easy and fast identification.

The objective of this work is to automate the teeth classification and numbering process in multi-slice CT (MSCT) images. In the previous work [19], we introduced a new technique by applying wavelet descriptors (WDs) for dental recognition in CT images which is not rotation invariant.

In this work, we present an algorithm to classify and assign numbers to teeth in MSCT images based on teeth contours. Our final goal is to utilize the algorithm in an automated dental recognition system. Contrary to previous works, we do not make any anatomical assumptions about the sequence and locations of the teeth in the jaw. In addition, selected features are invariant to geometrical transformation. The proposed algorithm consists of the following three stages: segmentation, feature extraction and classification.

The segmentation technique is based on our previous works and anatomical knowledge of dental arch [20,21]. We suggest a segmentation method using Otsu thresholding, morphological operations, panoramic re-sampling and variational level set in MSCT images. In the feature extraction stage, we introduce a multi-resolution method using Wavelet-Fourier descriptor (WFD) and employing a centroid distance signature. We apply a Wavelet transform (WT) to achieve a multi-resolution representation of the teeth shapes. We compute the feature vector of each tooth by employing the slice associated with largest tooth tissues. We utilize these coefficients in a conventional feed-forward neural network.

This paper is organized as follows. In "Proposed method" section, we propose techniques which are described in detail. Experimental results and comparison with previous methods are mentioned in "Experimental results" section. In "Discussion" section, we discuss about the results and performance of the proposed solutions. The paper ends with concluding remark and future steps, as mentioned in "Conclusion" section.

Proposed method

Dentistry requires several accurate assessments such as 3D measurements and representation of the teeth and jaws for diagnostic and treatment purposes. In this trend, volumetric CT data are the main source for dental practitioners and maxillofacial surgery. Teeth data might be acquired by conventional CT scanners and/or cone beam computed tomography (CBCT) imaging system [14]. Recently, the flat panel volumetric computed tomography (fpVCT) is a new CBCT device applicable to improve resolution in the imaging of human maxillofacial region [22].

We employed the following datasets in this research: teeth volumetric data sets were acquired by a SIMENS CT_SOM5 SPI System (CT SIMENS Sensation 64). CT images were acquired generally with a resolution of 512×512 pixels and 16 bits/pixels, 1 mm slice thickness and 0.8 mm inter-slice distance. Images were taken under the exposure condition of 120 kV and 81 mA. Data sets were collected from 30 different individuals, aged between 21 and 73 years.

We propose a multi-step approach for teeth numbering and classification. The proposed techniques are as follows: (1) Segmentation, (2) Feature extraction and (3) Classification. Figure 1 shows the block diagram of the techniques.

Segmentation

In dental CT data sets, in addition to teeth, other bony structures such as maxilla, mandible and cervical vertebra are also available. Conventional segmentation techniques are not appropriate to extract a tooth contour. In this regard, we propose a hybrid approach for teeth segmentation in MSCT images based on our previous works [20,21]. In the segmentation procedure, we apply an Otsu thresholding, morphological operations, panoramic re-sampling and variational level set in CT volumetric data. Segmentation procedures are shown in Fig. 1 and explained in the following.

Region of interest (ROI) localization

To speed up operations, a rectangular ROI in the middle slice of upper/lower jaw was manually adjusted to include all teeth throughout the jaw. Figure 2a and b illustrates a typical result.

Bony tissue separation

In the cropped images, we obtain a bony mask utilizing an Otsu thresholding [23] technique. In the available data

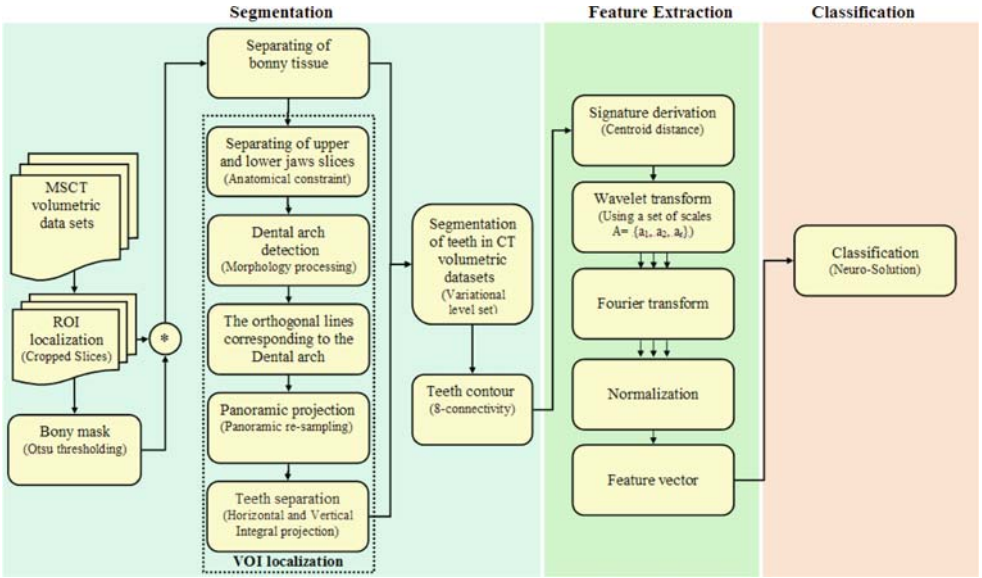

Fig. 1 Block diagram of teeth classification and numbering

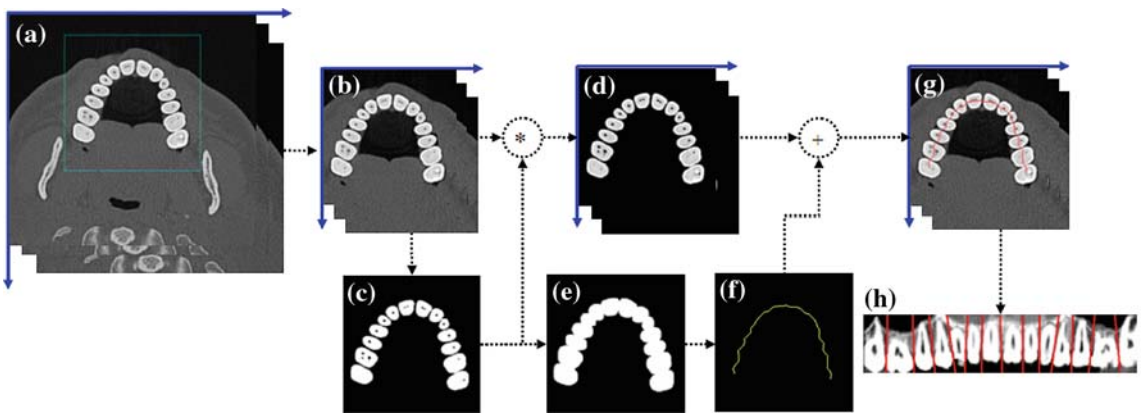

Fig. 2 Several steps of the proposed segmentation techniques. **a** A typical teeth CT image of the upper jaw. Rectangular region in the image is associated with the ROI. **b** Cropped image associated with ROI. **c** Extraction of bony mask by Otsu thresholding. **d** Separation of bony tissues from other tissues using bony mask. **e** Result of morphology processing (closing, dilation and filling). **f** Refined dental arch by a skeleton process. **g** Dental arch is overlaid with **d**. **h** Reconstructed panoramic image of the upper jaw is overlaid with refined projection lines

sets, due to high contrast of bony tissues with respect to soft tissues, Otsu's technique was successful to automatically determine needed threshold values. Resultant bony mask and tissues are given in Fig. 2c and d, respectively.

Volume of interest (VOI) localization

Based on the results obtained in previous step, we propose a technique to determine a volume of interest (VOI) for each tooth in the volume CT data. In this regard, we need to segment teeth from each other and jaws. In order to find an initial contour for teeth, we first estimate the dental arches [1] of the upper and lower jaws.

The CT images were acquired in open-bite condition. In this case, finding a slice without teeth is automatically possible and we can separate the upper and the lower jaws from each other. Sample line which is separating the mandible and maxilla is shown in Fig. 3.

As shown in Fig. 4a, in some cases, separation of teeth in upper and lower jaws with a straight line is not possible. In this case, based on a previous work in our group [24], in each row, we calculate the distance of the left edge of the image to the nearest bone pixel in that row. The row in which the mentioned distance is a maximum compared to the other rows a line is drawn from the left side of the image to the first bone pixel. From this pixel, a vertical line is drawn up till we reach the first bony pixel. On this vertical line the same procedure is performed which was performed on the left side of the image. This procedure is continued until we can no longer move right or upwards. This is illustrated in Fig. 4b. By seeing the result, we can clearly see that the teeth in the mandible and maxilla have been separated from each other. The result is shown in Fig. 4c.

We propose a morphology-based skeletonization to automatically estimate the dental arch. In this regard, we apply morphological operations (closing, dilation and filling) [25] to the bony mask obtained in previous steps. By this operation, possible gaps between teeth are effectively filled. Number of closing, dilation and filling were experimentally selected as one, three and one times, respectively. Then, by a skeleton-process we extract the longest line that is equidistant to the bone borders. Results of morphological operations and extracted skeleton are shown in Fig. 2e and f, respectively. We then estimate the orthogonal lines corresponding to arches of the upper and lower jaws. The volumetric CT data are then re-sampled with respect to these orthogonal lines and panoramic image of the data set is performed [20,21].

We separate the panoramic image into several blocks so that each block contains only one tooth. In this way, we define a VOI for each tooth. Separation of each tooth from its neighbors can be achieved utilizing the vertical lines. Details of these operations are given in [20,21]. Figure 2h shows the detected separating lines overlaid over the reconstructed panoramic image.

Segmentation of teeth in MSCT data set

In many dental CT slices, the gradient between the teeth and other bony tissues is not prominent and, hence, traditional techniques will not be able to accurately extract the tooth contour. To address this limitation, we utilize a variational level set method which derives the level set function by energy minimization [26]. Due to this characteristic, a variational level set method is able to detect a boundary. We employ a novel variational level set technique based on Mumford–Shah function [27] for segmentation. This model is able to detect contours with or without a gradient. Objects with smooth boundaries or even with discontinuous boundaries can be successfully detected. Moreover, the model is robust to the position of the initial contour. The 2D version of the model can be expressed as

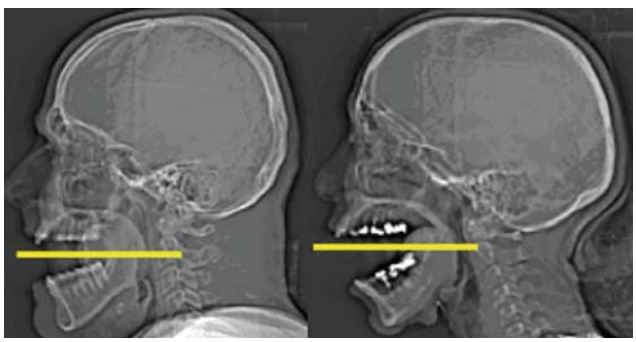

Fig. 3 Separation of mandible and maxilla in cases where a slice without teeth tissue is available in the data set

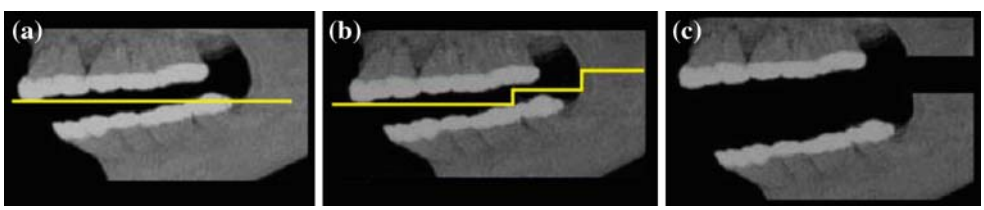

Fig. 4 The procedure for separating mandible and maxilla. **a** A straight line fails to separate teeth in the mandible and maxilla. **b** Estimated line-segments to separate teeth in the upper and lower jaws. **c** Final separated jaws

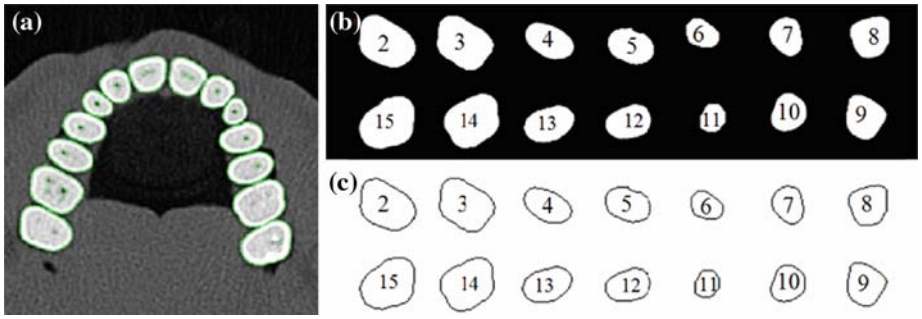

Fig. 5 Final segmentation result of a typical slice. **a** Refined boundaries of teeth contours (*green curves*) are overlaid with original image. **b** Mask of each individual tooth in image. **c** Universal number of each tooth are overlaid with mask (**b**) external contour is extracted by applying connected component analysis using external contour 8-connectivity

$$E(c_1,\ c_2,\ C) = \mu\,\text{Length}(C) + \nu\,\text{Area (Inside }(C)) + \lambda_1 \int_{\text{inside(C)}} (u_0(x,y) - c_1)^2\,\mathrm{d}x\,\mathrm{d}y + \lambda_2 \int_{\text{outside(C)}} (u_0(x,y) - c_2)^2\,\mathrm{d}x\,\mathrm{d}y, \quad (1)$$

where $u_0(x,\ y)$ is the original image, C_i are the averages of u_0 inside and outside C, $\mu \geq 0$ and, $\nu \geq 0$, and $\lambda_i \succ 0$ are fixed parameters. The level set function they obtain is given by

$$\frac{\partial \phi}{\partial t} = \delta(\phi)\left[\mu \text{div}\left(\frac{\nabla\phi}{|\nabla\phi|}\right) - \upsilon - \lambda_1 (u_0 - c_1)^2 + \lambda_2 (u_0 - c_2)^2\right] = 0, \quad (2)$$

where n denotes the exterior to the boundary $\partial\Omega$, and $\partial\phi/\partial n$ denotes normal derivative of ϕ at the boundary and $\delta(\phi)$ is the Dirac delta function that is the derivative of Heaviside function $H(\phi)$. Heaviside function defined by: $H(\phi) = 1$ if $\phi \geq 0$, and $H(\phi) = 0$ if $\phi \prec 0$.

We employ the initial boundaries performed in "VOI localization" to estimate the final contour of each tooth. In this regard, the VOI associated with each tooth can be relocated in the original CT volume. We utilze the results of proposed method by applying connected component analysis using 8-connectivity to extract the external contour of each tooth in image. Results are demonstrated in Fig. 5.[1]

Metal artifact reduction (MAR)

Metal artifact is a common distortion that degrades dental CT images. Metal artifact is generally caused by the presence of dental fillings or implants in the field of view (FOV) [28]. We employ a low-pass Butterworth filter and morphological operations (erosion, pruning, cleaning and opening) [25] to reduce metal artifacts [20,21]. Figure 6 represents the MAR technique utilized in segmentation procedures. As seen in Fig. 6, MAR is effective if accuracy of tooth segmentation is more than 90%. Otherwise, manual segmentation is employed in next operations.[2]

Feature extraction

Shape is an important visual feature and it is one of the basic features used to describe image content. In the literature, there are two categories for shape representation, i.e. region-based and contour-based, and each category has various methods with varying performance for different shapes. Region-based techniques consider whole area of the object while boundary based techniques concentrate merely on the boundary lines [29]. The boundary-based methods are more popular than region-based methods because the shape classifications are mainly attentive towards the contour features.

Fourier transform (FT) is one of the most popular techniques for shape analysis and description in the category of contour-based approach for more than four decades. The shape description and classification using Fourier descriptors (FDs) either in 1D or 2D space are invariant to the geometrical transformation like translation, rotation and scale, simple to compute, robust to noise, and compact, and it has many applications in different area, but it does not have a multi-resolution property [30,31].

In the past few years, wavelet transform (WT) has been widely used in the area of image processing and pattern classification because of its attractive multi-resolution, denoising

[1] The Adult dentition contains 32 teeth, 16 teeth in each jaw. In universal numbering system the two jaws divide into four equal quadrants that each quadrant contains eight teeth, two incisors, one cuspid (canine), two premolars (bicuspid), and three molars. the numbering system numbers permanent teeth from 1 to 32, beginning at the maxillary right third molar (#1), extending across the maxilla to the left third molar (#16), then continuing to the left mandibular third molar (#17), and going around the mandibular arch to the right third molar (#32).

[2] In the available data sets, segmented teeth of two experts with a similarity index of above 80% was employed as gold standard.

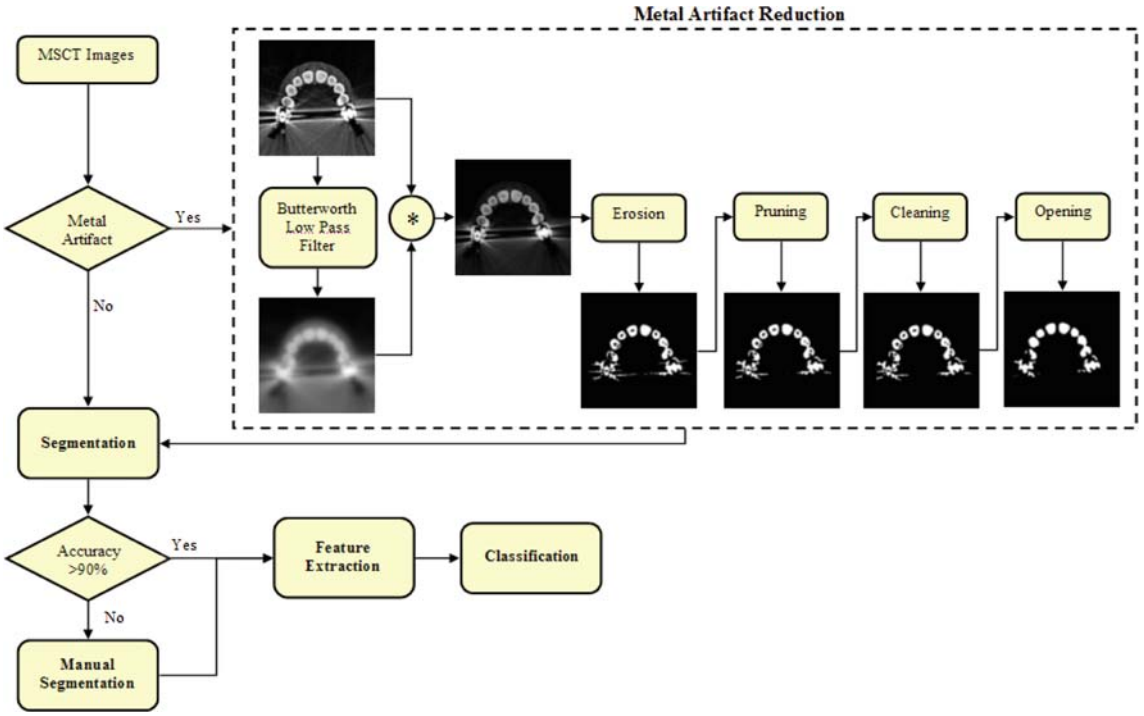

Fig. 6 MAR technique applied in teeth segmentation

and feature extraction capabilities. However, it has not been fully exploited for shape description. For describing complex shapes, it is required that shapes must be described at multiple resolutions. It has been reported that wavelet descriptors (WDs) are not translation and rotation invariant and also the matching scheme is more complicated and time consuming than that of FDs [32–34]. Therefore, we seek to use descriptors based on the teeth boundary that have better properties for recognition.

The proposed solution for mentioned problems is to apply the FT to the coefficients obtained from the WT. In this way, the multi-resolution shape representation can be transformed to the frequency domain, in which normalization and classification are straightforward operations. Hence, the benefits of multi-resolution representation and Fourier shape representation can be combined.

The multi-resolution representation of the object boundary can be achieved using WT. The boundary function is transformed using some wavelet ψ. WDs are coefficients of WT to the boundary function of an object. Wavelet-based methods are ideally suited for highlighting local features in the decomposed sub-images. WDs are formed on the basis of wavelet representation of the original sequence, which describes the boundary of the shape. The wavelet coefficient of the image boundary $r(t)$ at a scale a and position b is defined as follows:

$$C_a(b) = \frac{1}{\sqrt{|a|}} \int_R r(t)\psi\left(\frac{t-b}{a}\right) \mathrm{d}t. \tag{3}$$

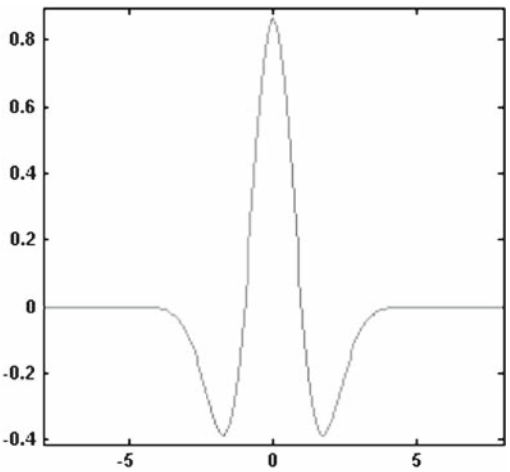

Fig. 7 Mexican-hat wavelet function [35]

In the case of WT we obtain a set of coefficients $C_a(b)$ of scale a. The coefficients are defined for all positions $b = 0, 1, 2, \ldots, N-1$. In the experiment of this paper we have used Mexican-hat wavelet [35], which is the second derivative of the Gaussian wavelet. Figure 7 shows the Mexican-hat wavelet function, which is represented as

$$\psi(t) = \left(\frac{2}{\sqrt{3}}\pi^{-1/4}\right)\left(1-t^2\right)e^{-t^2/2}. \tag{4}$$

In shape description, a boundary is usually presented using some shape signature such as complex coordinates, centroid

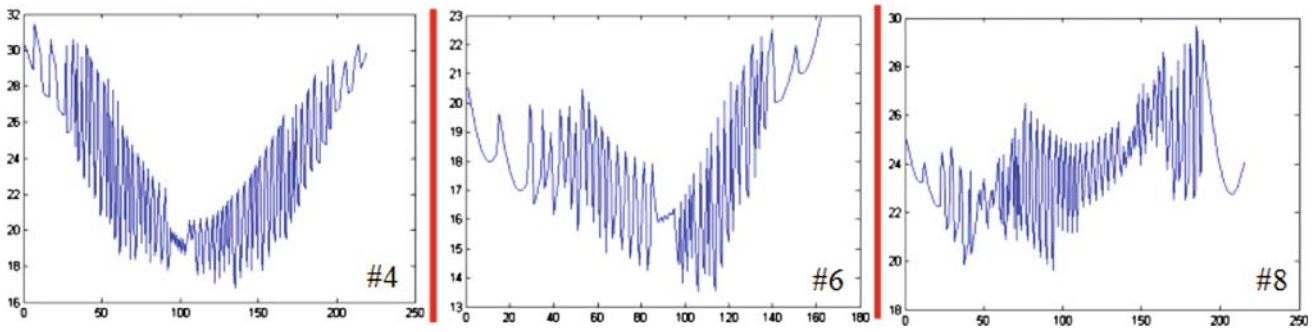

Fig. 8 Centroid distance signature of several teeth (#4, #6 and #8)

distance, cumulative angular function and curvature signature [29]. A shape signature is any 1D representation of 2D areas or boundaries. The centroid distance function is expressed by the distance of the boundary points from the centroid $(x_c,\ y_c)$ of the shape,

$$r(t) = \left([x(t) - x_C]^2 + [y(t) - y_C]^2\right)^{1/2}, \tag{5}$$

where $x_C = \frac{1}{N}\sum_{n=0}^{N-1} x(t)$ and $y_C = \frac{1}{N}\sum_{n=0}^{N-1} y(t)$.

Due to the subtraction of centroid, which represents the position of the shape from boundary coordinates, the centroid distance is invariant to translation. For this reason, we employed centroid distance based shape signatures. The centroid distance of some teeth has been shown in Fig. 8. It shows that each class tooth has a unique shape signature which causes more tolerant power for the derivation of feature descriptors.

The problem with the coefficients obtained from the WT is the fact that they are dependent on the starting point of the object boundary. Hence the obtained descriptor is not rotation invariant. Also the dimensionality of the feature vector depends on the boundary length. Therefore, the coefficient vectors of different shapes cannot be directly used in the image classification. FDs characterize the object shape in a frequency domain. Wavelet-Fourier descriptors (WFDs) [36,37] are the selected coefficients obtained after applying the FT to the wavelet coefficients $C_a(b)$ and is defined as

$$F^a(s) = \frac{1}{N}\sum_{b=0}^{N-1} C_a(b)\exp(-j2\pi b/N), \quad s = 0, 1, 2, \ldots, N-1. \tag{6}$$

The FT of the Mexican-hat wavelet function is real valued and symmetrical. Due to use of centroid distance shape signature, the WFD are invariant to the translation effect. For the rotation invariance, the phase part is discarded and only the magnitude part of the feature vectors is used. The feature vectors are normalized to achieve the scale invariance. In this way, the WFD is made invariant to translation, rotation, and scale. The multi-resolution descriptor f^a of each scale a is then formed from coefficients $F^a(s)$ in the following invariant feature vector:

$$f^a = \left[\frac{|F^a(1)|}{|F^a(0)|}, \frac{|F^a(2)|}{|F^a(0)|}, \ldots, \frac{|F^a(N-1)|}{|F^a(0)|}\right]^T. \tag{7}$$

The multi-resolution representation of the object shape can then be formed by defining the descriptor f^a using several different scales a, and combining the descriptors into a single feature vector. If the set of scales is defined as $A = \{a_1, a_2, \ldots, a_r\}$, the number of the scales in the descriptor is r. The dimensionality of the obtained feature vector is $r*L$. The outline of the employed method is illustrated in the feature extraction stage of Fig. 1.

Classification

Different types of neural networks have been applied in pattern recognition problems. They include the multilayer perceptron (MLP), Kohonen self-organizing network and hybrid structure composed of the self-organizing layer and the MLP sub-network connected in cascade. The MLP is a feed-forward network structure in which neurons are connected only between two succeeding layers [38].

We utilize a conventional supervised classifier for teeth identification. The recognition is based on the features extracted from the wavelet-Fourier transformations of the data, describing the shape of the pattern. We employ a feed-forward neural network classifier to discriminate different teeth from each other. In this regard, we experimentally found that a feed-forward neural network with one hidden layer and a transfer function of 'tansig' was suitable for undertaking the task [19]. The classification is done by Neuro-Solutions for Excel in which the training, testing and validation data are selected in whole data set and in an automatic way. Neuro-Solutions simulations are vector based for efficiency. This implies that each layer contains a vector of processing elements (PEs) and that the parameters selected apply to the entire vector. The parameters are dependent on the neural model, but all require a nonlinearity function to specify the behavior of the PEs. In addition, each layer has an associated

Table 1 Available teeth in 30 MSCT data sets

Teeth class	Upper jaw (maxilla)		Lower jaw (mandible)	
	Teeth no.	Total number of each type	Teeth no.	Total number of each type
Anterior				
Incisor	#7, #8, #9, #10	107	#23, #24, #25, #26	118
Canine	#6, #11	58	#22, #27	60
Posterior				
Premolar	#4, #5, #12, #13	108	#20, #21, #28, #29	88
Molar	#1, #2, #3, #14, #15, #16	145	#17, #18, #19, #30, #31, #32	120

Table 2 Performance measure of proposed method and a previous work [21]

Measure (%)	Definition	A previous work [21]	Proposed method
Sensitivity	TP/(TP + FN)	84.25	87.99
Specificity	TN/(TN + FP)	95.62	99.30
Precision	TP/(TP + FP)	87.80	93.09
Accuracy	(TP + TN)/(TP + TN + FP + FN)	92.00	98.42
Mean error rate	(FP + FN)/(TP + TN + FP + FN)	4.4612	1.7125

learning rule and learning parameters. The numbers of PEs and learning parameters are entered in the corresponding fields. The learning rule and nonlinearity are selected from a list of options contained. Note that the number of PEs for the Output Layer is determined by the number of columns selected as one's desired response [39].

Experimental results

The proposed method was evaluated in the presence of 30 MSCT cases including 804 teeth. Most cases were admitted for dental implant procedures. Available teeth are shown in Table 1. We implemented the techniques by MATLAB [40] using a Pentium IV CPU (3.00 GHz-Dual Core) on a Microsoft Windows XP environment.

Using the technique proposed in "Segmentation" section, a dental arch was extracted within 1.8 s. The tooth contours were then performed by panoramic re-sampling and employed as initial boundary for the variational level set. The teeth segmented by the proposed methods were also compared with those manually segmented by the expert. In order to validate the proposed segmentation methods, the sensitivity, specificity, precision, accuracy and mean error rate were calculated [41]. For this purpose, true positive (TP), false positive (FP), true negative (TN) and false negative (FN) values were computed. Table 2 shows these parameters for the proposed method and a previous work [21] in the presence of the available data sets.

The receiver operating characteristic (ROC) of the proposed and previous [21] works are shown in Fig. 9. As seen, the proposed technique outperforms the previous work.

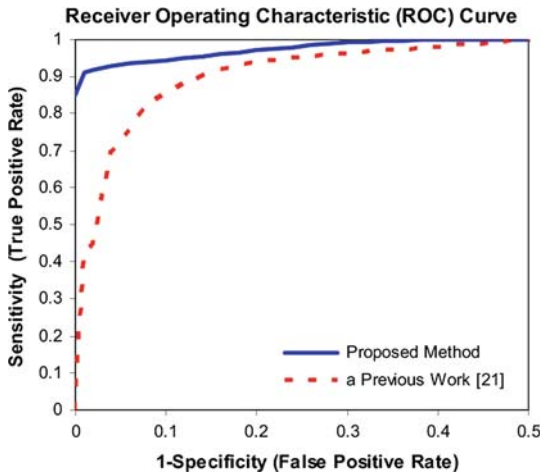

Fig. 9 The ROC curves of the proposed and previous [21] works

In Fig. 10, segmented teeth are typically visualized by a marching cubes (MC) algorithm [42] employing a VTK library [43].

In classification step, we computed the feature vector of each tooth by only employing the slices associated with clinical-crown in the dataset. We experimentally found that such slices are very effective in teeth classification. This is illustrated in Fig. 11.

In the multi-resolution WFD approach, FT is applied to the coefficients of WT of the boundary signature function. Therefore, the shape information in form of feature vectors is found in frequency domain. Because the wavelet coefficients of a shape signature have multi-resolution representation of the original shape signature, we apply a coarse-to-fine

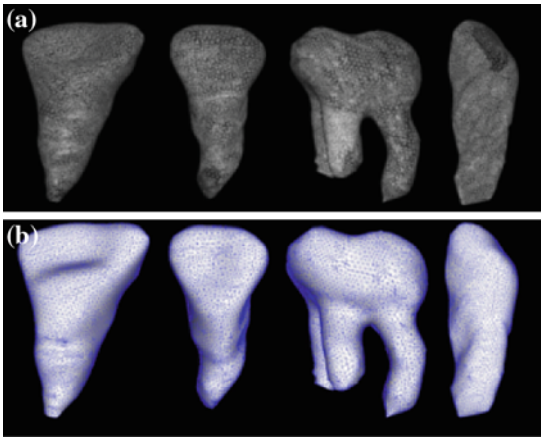

Fig. 10 Typical teeth (#8, #10, #15 and #27) are visualized by (**a**) a Delaunay triangulation, (**b**) a MC algorithm using the VTK library

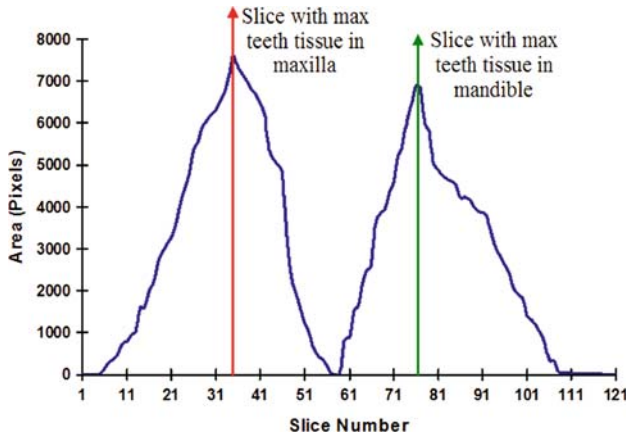

Fig. 11 Teeth area for every slice in a typical data set by proposed segmentation method

strategy. The coarse scale Wavelet coefficients normally represent the global feature of the signature, while the fine scale coefficients represent the details of the signature. Due to noise introduced in the original image and the errors accumulated, the detail coefficients were found less important than the coarse scale coefficients. To reduce the dimensionality of the features, the number of scales was selected to be low in the multi-resolution approaches. In the classification stage, the scale set a was selected to be [4,16]. The inverse relationship between time and frequency is shown in Fig. 12. After applying Fourier transform operation to the wavelet coefficients of image, we obtain a large numbers of WFD coefficients. There are two levels of frequency descriptors: low- and high-frequency descriptors. The low-frequency descriptors have the details of the general features, while high-frequency descriptors contain finer details of the object. Out of these coefficients, some are significant for teeth classification, which are also known as the representative of the contour. The sets of features for these images were generated

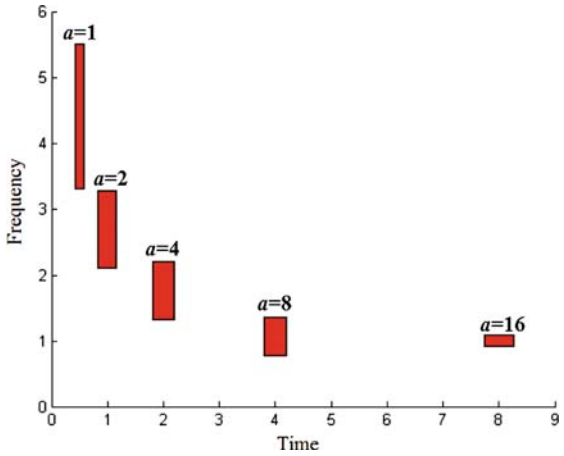

Fig. 12 Time–frequency boundaries of the Mexican hat wavelet for various values of a

and a feed-forward neural network with one hidden layer was trained by employing 50% of the teeth in the data set.

The *classification performance rate* ($\eta\%$) technique [37] was employed as evaluation scheme. The classification performance is a metric, which we used to evaluate the classification experiment conducted for shape-based objects. It is defined as

$$\eta = \frac{m-n}{m} \times 100, \tag{8}$$

where m is the total number of classified image and n the total numbers of misclassified images. The rates allow us to assess the performance of proposed method in the presence of different classes of teeth. Table 3 shows the classification performance rate of our classification method in a typical CT dataset. The results show a considerable change in performance. The maximum change is in the performance of the premolars in the mandible. The experiments show that the classification of premolars in both jaws is more difficult than other teeth. In addition, we experimentally found that classification of teeth in mandible is more difficult than maxilla.

The classification performance of the proposed methods are tested and compared with FDs and WDs technique, which are introduced in [12] and [19], respectively. The average classification performance for different type of teeth has been shown in Fig. 13 using FDs, WDs, and WFDs techniques. It is inferred that the WFD technique performs better than FD and WD for whole data set classification. The classification performances are above 94% in all class of teeth.

We also carried out the experiment to check the invariance properties. Because translation dose not change the relative position of the centre of mass of a tooth contour, our major concern is the system's performance on rotation and scaling. For each tooth, we tested six rotation angles and six scaling factors. The six rotation angles (θ) are 45, 90, 135, 180, 225,

Table 3 Typical classification performance rate ($\eta\%$) of teeth in Maxilla and mandible using WFDs

Teeth class	Upper jaw (maxilla)		Lower jaw (mandible)	
	Teeth no.	Classification performance, η (%)	Teeth no.	Classification performance, η (%)
Anterior				
Incisor	#7	99.37	#23	98.15
	#8	100	#24	98.00
	#9	100	#25	100
	#10	99.12	#26	98.47
Canine	#6	100	#22	98.39
	#11	99.07	#27	98.04
Posterior				
Premolar	#4	98.21	#20	97.70
	#5	98.87	#21	97.41
	#12	98.92	#28	97.93
	#13	98.73	#29	97.55
Molar	#2	100	#18	100
	#3	99.82	#19	98.10
	#14	100	#30	99.81
	#15	99.69	#31	98.05

In this typical data set there is not exist wisdom teeth (#1, #16, #17, #32)

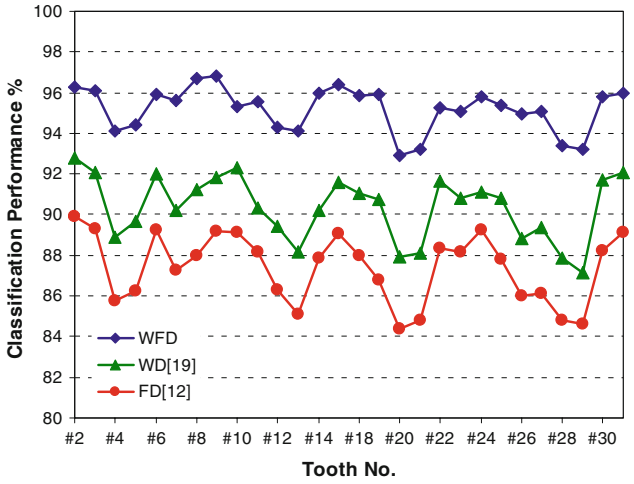

Fig. 13 Average classification performance of different teeth type using WFD, WD [19] and FD [12] techniques

270 and 315°, and the seven different scaling factors (SF) are 0.4, 0.6, 0.8, 1.2, 1.4, 1.6 and 1.8. A typical molar tooth (#2) in different rotation angles and scaling factors is shown in Fig. 14. We get 100% recognition rate for all the rotation angles and scaling factors. These results demonstrate the effectiveness of proposed algorithm against a previous work [19].

We used additive Gaussian noise to the centroid distance signature of teeth contours to study the effect on classification performance. Since the main parameters for noise study are mean μ and standard deviation σ^2, we studied the effect after applying of constant value of mean and different values of variance. The experiment with constant value of mean and different values of variance was observed that the noisy teeth images were classified. Figure 15 shows a typical incisor (#9) images with additive Gaussian noise with constant value of $\mu = 0$ and different values of variances $\sigma^2 = 0.2, 0.4, 0.6$, in which the classification performance is 100, 100 and 96%, respectively.

The CPU time for different steps of the proposed method is illustrated in Table 4.

Discussion

The proposed work of this research is based on a multi-step approach. Compared to a previous work [21], bone tissue separation was performed by an Otsu's technique. In this case, the proposed technique outperformed the previous approach (level set technique) in term of speed and automatic selection of threshold values. As the result of a variational level set algorithm, that was employed both in the proposed and

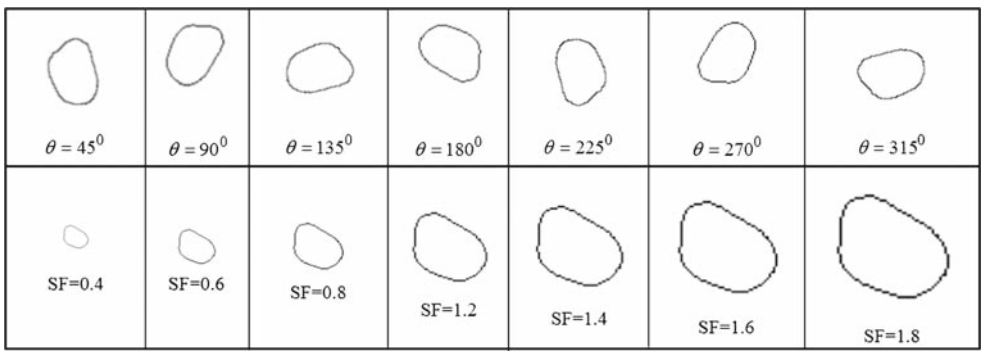

Fig. 14 Some training image of a typical molar (#2) in different rotation angles and scaling factors

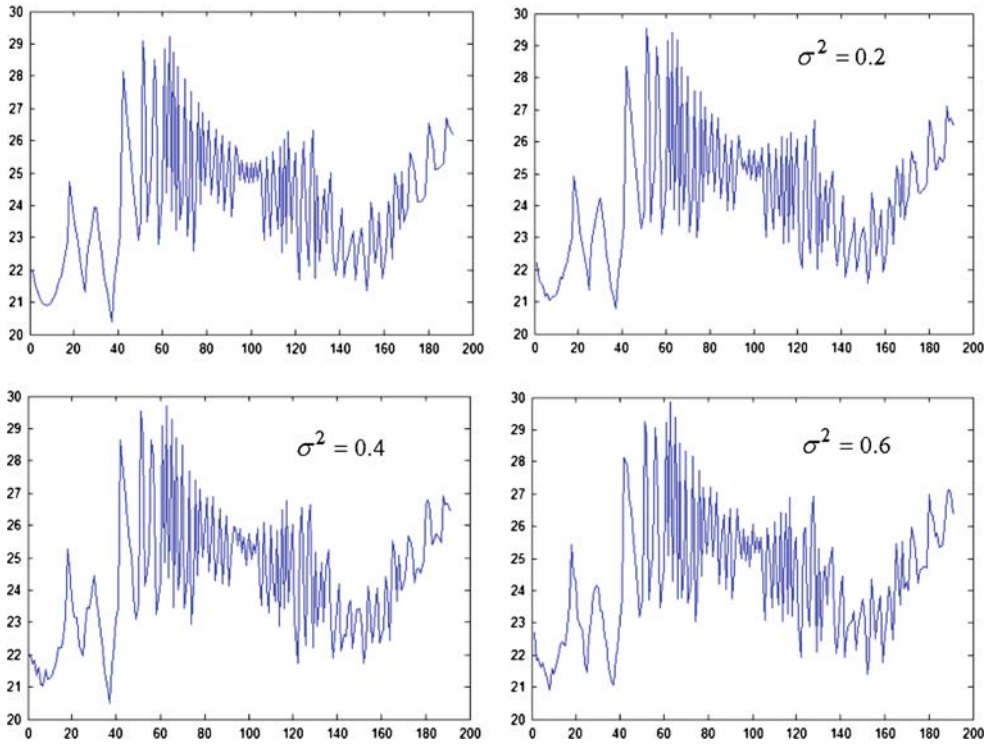

Fig. 15 Some training centroid distance signature of a typical incisor (#9) which affected by Gaussian noise

Table 4 Elapsed time for different stages of proposed methods

Stage	Time
Segmentation	5–8 min
Feature extraction	1–2 min
Classification	90–96 ms

previous work, depends on good initial contour, final segmented tooth in the proposed method was of higher quality.

In this paper, we have used contour-based descriptors. FDs characterize the object shape in a frequency domain. WDs have short-time resolution for high frequencies and long-time resolution for low frequencies because of their multi-resolution property. Applying Fourier transform to the wavelet coefficients the benefits of multi-resolution representation and Fourier shape representation are combined that yields better performance. WFD provide good classification performance when only a small number of scales are used. Therefore, WFD provides additional margin as compared to the FD and WD, which provided additional accuracy for invariant shape classification.

An essential matter of the usability of the proposed WFDs is their capability of being used in teeth recognition system. In this study, WFDs derived from centroid distance signature. Because of the property that centroid distance captures both local and global features of shape makes it desirable as shape representation. It is robust and information preserving. The proposed WFD considers the shapes in multiple scales, which make them more insensitive to fine details in the shape boundary than the FDs. The hierarchical coarse-to-fine representation is related to classification performance. In the classification process, clearly dissimilar teeth can be eliminated at coarse level, whereas detailed matching is performed at finer levels. This kind of representation can be achieved by selection of the number of the Fourier coefficients and scales. Coarse representation can be obtained using only a few low-frequency coefficients and scales. When their number is increased, the representation is finer and the shape is characterized in more details in the descriptor. The WFD technique has very good shape classification accuracy in the case of rotated, translated and scaled shapes. It is also robust to noise.

The major misclassification that might be seen in image is related to the mirror of the corresponding tooth in jaws. The main reason is because of the inherent similarity between teeth signature. Because of this reason, a better quality of implant can be obtained by using the mirror image of the corresponding tooth on the other side of the jaw to define a 3D representation of the missing tooth. In practice, in real images, we have different kinds of errors and imprecision due to the fact that images are characterized by a large amount of sensorial noise due to the acquisition system. Also computational noise must be taken into account, in particular due to discrete acquisition and interpolation. We found that, between sensorial noise, the noise due to metallic reflection is a major obstacle in teeth classification and numbering.

Compared to [12] and [19], the method is independent of anatomical information such as knowing the sequence of teeth, the approximated location of each tooth in the mouth and with respect to each other. Contrary to previous work [19], all achieved features invariant to scale, translation, and rotation.

Conclusion

In this paper, we have proposed a method for automatic classification and numbering of teeth in MSCT images using a multi-stage algorithm. Our method is independent of anatomical information such as knowing the sequence of teeth, the approximated location of each tooth in the mouth and with respect to each other.

We segmented the teeth by a hybrid approach based on our previous experiences and anatomical knowledge of dental arch. A variational level set technique was used to extract the contour of teeth from dental images. The proposed algorithm was applied to extract the tooth contour using a technique that depends on the intensity of the whole tooth region and not just the edges. Experimental results confirmed the efficiency of the contour extraction process using the proposed technique.

We have employed a multi-resolution WFD, which derived from centroid distance shape signature. In the WFD methodology, FT is applied to the coefficients of WT of the boundary signature function. Therefore, the shape information in form of feature vectors is found in frequency domain. The recognition was based on the features extracted from the wavelet-Fourier transformations of the data, describing the shape of the pattern. We utilized a conventional supervised classifier for teeth identification. We employ a feed-forward neural network classifier to discriminate different teeth from each other. We achieved a high classification performance rate for all different type of teeth and rotation angles and scaling factors.

The plan for future work includes combining the information of dental root with dental crown to reach higher classification performance. Future work can also be done for recognizing teeth in more data sets and different imaging conditions and different modalities such as datasets acquired by cone beam CTs. Considering anatomic variations and dental anomalies needs further modification and evaluation of the proposed technique. Building teeth generic shape models for computer-assisted surgical planning is another future challenge.

References

1. Fuller J, Denehy G (2001) Concise dental anatomy and morphology. The University of Lowa press, Ames
2. Pongrdcz F, Bdrdosi Z (2006) Dentition planning with image-based occlusion analysis. Int J CARS 1:149–156. doi:10.1007/s11548-006-0052-6
3. Valente F, Sbrenna A, Buoni C (2006) CAD CAM drilling guides for transferring CT-based digital planning to flapless placement of oral implants in complex cases. Int J CARS 1:413–426. doi:10.1007/s11548-006-0025-9
4. Eggers G, Kress B, Fiebach J, Rieker M, Spitzenberg D, Ghanai S, Marmulla R, Muhling J, Dickhaus H (2006) MRI-based creation of jaw models for therapy planning. Int J CARS 1:427–435. doi:10.1007/s11548-006-0035-7
5. Yoo K, Ha J (2005) An effective modeling of single cores prostheses using geometric techniques. Comput Aided Des 37:35–44
6. Bossard D, Dubos N, Trunde F, Huet A, Coudert JL (2004) 3D computed-assisted surgery in orthodontic treatment of impacted canines in palatal position. Int Congr Ser 1268:1203–1208
7. Jain AK, Chen H (2004) Matching of dental X-ray images for human identification. J Pattern Recognit 37:1519–1532
8. Nomir O, Abdel-Mottaleb M (2005) A system for human identification from X-ray dental radiographs. J Pattern Recognit 38:1295–1305
9. Zhou J, Abdel-Mottaleb M (2005) A content-based system for human identification based on bitewing dental X-ray images. J Pattern Recognit 38:2132–2142
10. Sidler M, Jackowski C, Dirnhofer R, Vock P, Thali M (2006) Use of multislice computed tomography in disaster victim Identification-Advantages and limitations. Forensic Sci Int 38:2132–2142
11. Murray D, Whyte A (2002) Dental panaromic tomography: what the general radiologist needs to know. Clin Radiol 57:1–7
12. Mahoor MH, Abdel-Mottaleb M (2005) Classification and numbering of teeth in dental bitewing images. Pattern Recognit 38:577–586
13. Jain AK, Chen H (2005) Registration of dental atlas to radiographs for human identification. In: Proceedings of international society for optical engineering (SPIE), Conference on Biometric Technology for human Identification, vol 5779. Orlando, pp 292–298
14. Scarfe WC, Farman AG (2006) Clnical application of cone-beam computed tomography in dental practice. J Can Dent Assoc 72:75–80
15. Kirchhoff S, Fischer F, Lindemaier G, Herzog P, Kirchhoff C, Becker C, Bark J, Reiser MF, Eisenmenger W (2008) Is post-mortem CT of the dentition adequate for correct forensic identification? comparison of dental computed. Int J Legal Med 122:471–479
16. Jackowski C, Aghayev E, Sonnenschein M, Dirnhofer R, Thali MJ (2006) Maximum intensity projection of cranial computed tomography data for dental identification. Int J Legal Med 120(3):165–167
17. Jackowski C, Lussi A, Classens M, Kilchoer T, Bolliger S, Aghayev E, Criste A, Dirnhofer R, Thali MJ (2006) Extended CT scale overcomes restoration caused streak artifacts for dental identification in CT-3D color encoded automatic discrimination of dental restorations. J Comput Assist Tomogr 30(3):510–513
18. Thali MJ, Markwalder T, Jackowski C, Sonnenschein M, Dirnhofer R (2006) Dental CT imaging as a screening tool for dental profiling: advantages and limitations. J Forensic Sci 51(1):113–119
19. Momeni M, Zoroofi RA (2008) Automated dental recognition by wavelet descriptors in CT multi-slices data. Int J CARS 3:533–542. doi:10.1007/s11548-008-0255-0
20. Hosntalab M, Zoroofi RA, Abbaspour Tehrani-Fard A, Shirani G (2008) Segmentation of teeth in CT volumetric data set by panoramic projection and variational level set. Proc 22nd Int Congress and Exhibition CARS, p S442. doi:10.1007/s11548-008-0208-7
21. Hosntalab M, Zoroofi RA, Abbaspour Tehrani-Fard A, Shirani G (2008) Segmentation of teeth in CT volumetric data set by pano-

ramic projection and variational level set. Int J CARS 3(3–4):257–265. doi:10.1007/s11548-008-0230-9
22. Baba R, Ueda K, Okabe M (2004) Using a flat-panel detector in high resolution cone beam CT for dental imaging. Dentomaxillofac Radiol 33(5):285–290
23. Otsu N (1979) A threshold selection method from gray-level histograms. IEEE Trans Syst Man Cybern 9(1):62–66
24. Akhoondali H, Zoroofi RA (2009) Rapid automatic segmentation and visualization of teeth in CT-scan data. J Appl Sci 9(11):2031–2044. doi:10.3923/jas.2009.2031.2044
25. Gonzales R, Woods R (2002) Digital image processing, 2nd edn. Prentice Hall, New Jersey
26. Zhao HK, Chan TF, Merriman B, Osher S (1996) A variational level set approach to multiphase motion. J Comput Phys 127(1):79–195
27. Vese L, Chan T (2002) A multiphase level set framework for image segmentation using the Mumford and Shah model. Int J Comput Vision 50(3):271–293
28. Strumas N, Antonyshyn O, Yaffe MJ, Mawdsley G, Cooper P (1998) Computed tomography artefacts: an experimental investigation of causative factors. Can J Plast Surg 1:23–29
29. Zhang D, Lu G (2004) Review of shape representation and dscription techniques. Pattern Recognit 37:1–19
30. Zahn CT, Roskies RZ (1972) Fourier descriptors for plane closed curves. IEEE Trans Comput 21(3):269–281
31. Persoon E, Fu K-S (1977) Shape discrimination using Fourier descriptors. IEEE Trans Systems Man Cybern (SMC) 7:170–179
32. Chang GC, Kuo CCJ (1996) Wavelet descriptor of planer curves: theory and applications. IEEE Trans Image Process 5:56–70
33. Tieng QM, Boles WW (1997) Recognition of 2D object contours using the wavelet transform zero-crossing representation. IEEE Trans Pattern Anal Mach Intell 19(8):910–916
34. Yang HS, Lee SU, Lee KM (1998) Recognition of 2-D object contours using starting-point independent wavelet coefficient matching. J Vis Commun Image R 9:171–181
35. Misiti M, Misiti Y, Oppenheim G, Poggi JM (2007) Wavelets and their applications, 1st edn. ISTE Ltd, London
36. Chen G, Bui TD (1999) Invariant Fourier-wavelet descriptors for pattern recognition. Pattern Recognit 32:1083–1088
37. Yadav RB, Nishchal NK, Gupta AK, Rastogi VK (2007) Retrieval and classification of shape-based objects using Fourier, generic Fourier, and wavelet-Fourier descriptors technique: A comparative study. Opt Lasers Eng 45:695–708
38. Osowski S, Nghia DD (2002) Fourier and wavelet descriptors for shape recognition using neural networks-a comparative study. Pattern Recogniti 35:1949–1957
39. http://www.neurosolutions.com
40. http://www.mathworks.com
41. Fawcett T (2006) An introduction to ROC analysis. Pattern Recognit Lett 27(8):861–874
42. Newman TS, Yi H (2006) A survey of the marching cubes algorithm. Comput Graph 30(5):854–879
43. http://www.vtk.org